Eidgenössische Technische Hochschule Zürich
Swiss Federal Institute of Technology Zurich

Institute for Atmospheric and Climate Science

Master Thesis Proposal

Effect of resolving convection in the Integrated Forecasting System on the representation of a warm conveyor belt

ETH Zürich
Departement Environmental Systems Science
Institute for Atmospheric and Climate Science

Supervision

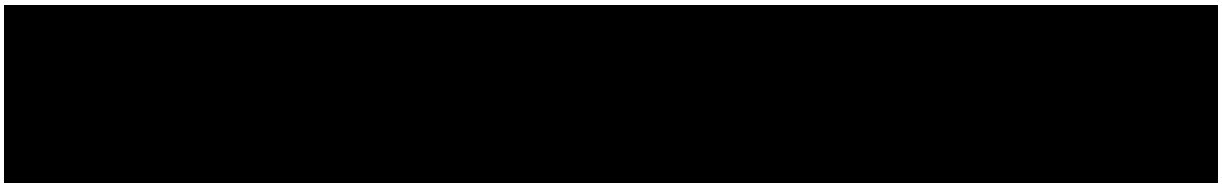

Submitted by

Zurich, May 26, 2020

Summary

Warm conveyor belts (WCBs) are coherent airstreams in extratropical cyclones that ascend from the planetary boundary layer to the upper troposphere within two days. They are the primary cloud and precipitation-producing flow in extratropical cyclones. Diabatic processes in the WCB lead to local heating and cooling. Thereby, they influence the dynamics of the extratropical cyclone and interact with the downstream Rossby wave pattern. Convection embedded in a WCB frequently occurs and modifies the precipitation pattern and influences the dynamics of the extratropical cyclone. Convection-permitting models are needed to simulate convection in a WCB explicitly. Until now, most global models use a parameterization scheme for convection. Hence, convection in WCBs was only explicitly studied with regional convection-permitting models, which can be run at a higher resolution. Recently, the European Centre for Medium-Range Weather Forecasts performed global simulations on the kilometer scale with a convection-permitting version of the Integrated Forecasting System (IFS). In this master thesis, we will investigate the influence of model resolution in global simulations of the IFS on a WCB. We will calculate trajectories based on a forecast with the operational IFS model and a simulation with the non-hydrostatic option of the IFS and systematically compare both forecasts. The calculated WCB trajectories will provide better knowledge of the influence of convection embedded in a WCB on the WCB itself, its precipitation pattern, and the flow evolution downstream.

Contents

1 Introduction

Extratropical cyclones are an essential component of mid-latitude weather and strongly influence the climate. In a frame of reference following an extratropical cyclone, Carlson (1980) identified different discrete airstreams (Fig. 1). These are (1) the warm conveyor belt (WCB), which is the primary cloud- and precipitation-producing flow (e.g., Browning, 1986; Eckhardt et al., 2004; Pfahl et al., 2014), (2) the cold conveyor belt, a secondary cloud-producing flow (Browning, 1986), and (3) the dry intrusion, a descending airstream from the upper levels west of the trough (e.g., Carlson, 1980; Young et al., 1987). In a WCB, the air is transported from the atmospheric boundary layer in the cyclone's warm sector upward and typically poleward (e.g., Wernli and Davies, 1997; Stohl, 2001; Madonna et al., 2014). This diabatic and cross-isentropic ascent to the tropopause takes place in approximately two days and connects the atmospheric boundary layer with the upper troposphere (e.g., Wernli and Davies, 1997; Stohl, 2001).

During its ascent, a WCB forms liquid and mixed-phase clouds as well as cirrus clouds in its outflow region (Madonna et al., 2014). These clouds form precipitation, and in many regions in the extratropics, WCBs contribute a large part to total precipitation (Pfahl et al., 2014). This is the case even though WCBs occur less than 10% of the time in all regions (Madonna et al., 2014). WCBs influence even more extreme precipitation events, and over some regions, WCBs accompany more than 70% of the extreme precipitation events (Pfahl et al., 2014).

The formation of clouds and precipitation is linked to strong diabatic processes that can influence the dynamics. In the framework of potential vorticity (PV), diabatic processes in a

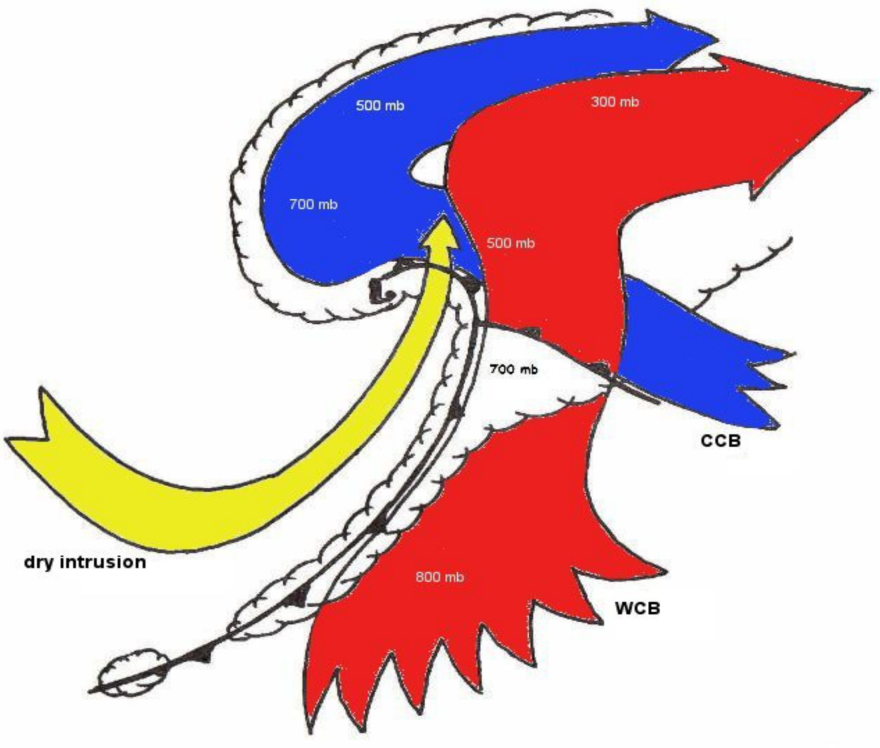

Figure 1: Schematic model of airstreams in an extratropical cyclone. Shown are the cold and warm front as well as the warm conveyor belt (WCB, red), the cold conveyor belt (CCB, blue) and the dry intrusion (yellow). The numbers give the approximate height of the airstreams in millibars (from Carlson, 1991).

WCB modify the distribution of PV (Wernli and Davies, 1997). It is frequently assumed that the vertical gradient of diabatic heating in large-scale WCB ascent is dominant for the change of PV and that the horizontal terms can be neglected (e.g., Wernli and Davies, 1997; Joos and Wernli, 2012; Madonna et al., 2014). Considering only the vertical terms of PV tendency leads to PV production below and PV destruction above the diabatic heating maximum. Dependent on (1) the upper-level forcing for ascent, (2) the strength of the WCB, and (3) its location, this low-level positive PV anomaly can lead to cyclone intensification (Binder et al., 2016). The typically low PV values of the WCB outflow generate a negative upper-level PV anomaly that can modify the large-scale flow evolution (Pomroy and Thorpe, 2000; Grams et al., 2011; Joos and Wernli, 2012; Joos and Forbes, 2016; Martínez-Alvarado et al., 2016). In some cases, these negative upper-level PV anomalies amplify the ridge (Pomroy and Thorpe, 2000) and favor downstream Rossby wave breaking and the development of stratospheric PV streamers (Grams et al., 2011).

In the last century, Harrold (1973) first described the WCB as a continuously rising and stratiform cloud-producing airstream. Nonetheless, Browning (1971) observed small-scale convection modifying the large-scale ascent within the WCB. Based on radar measurements, he found that the convection in the WCB tends to exist in mesoscale clusters aligned in bands. Figure 2 shows a model where the convection appears predominantly ahead of the cold and warm front. Later, Neiman et al. (1993) introduced the escalator-elevator concept of a WCB, where slantwise ascent (escalator) alters spatially with faster convective ascent (elevator). Recent studies (Binder et al., 2016; Crespo and Posselt, 2016; Flaounas et al., 2016; Rasp et al., 2016; Flaounas et al., 2018; Oertel et al., 2019) confirmed, at least for some case studies, this concept and showed that convection is regularly embedded in a WCB. Oertel et al. (2019) corroborated, based on trajectory calculations and satellite products, that embedded convection occurs predominantly as line convection in the vicinity of the surface cold front. They could also recognize deep convective clouds in the southern part of the warm sector and north of the cyclone center. In contrast to isolated convection, comparatively low values of convective available potential energy, weak lightning activity, and low updraft velocities characterize embedded convection in a WCB (Oertel et al., 2019). Nonetheless, the stronger updrafts allow for graupel formation, and the convective ascent causes a denser cloud structure (Oertel et al., 2020).

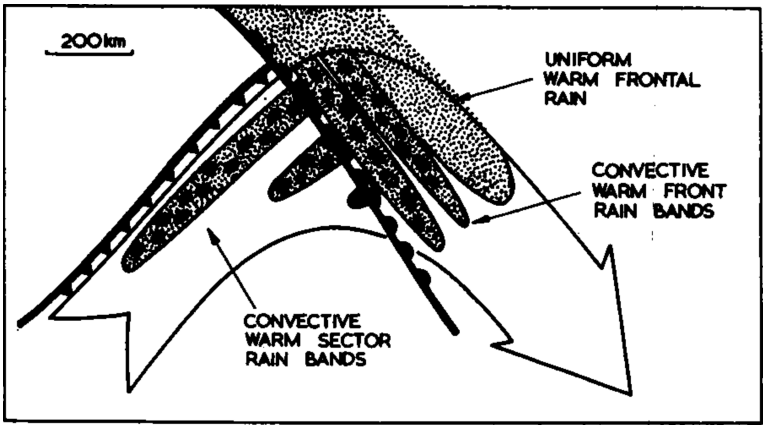

Figure 2: Model of precipitation associated with a WCB. The arrow denotes the WCB. The extent of moderate and heavy rain is represented by stippled and hatched shading, respectively. Clusters of convective cells with heavy precipitation are aligned in bands ahead of the cold and warm front (from Browning, 1971).

Moreover, convection embedded in WCBs is vital for intense surface precipitation and produces localized precipitation peaks (Oertel et al., 2019).

Convective updrafts embedded in the slantwise ascent of the WCB lead, apart from vertical gradients, to horizontal gradients of diabatic heating. Under these circumstances, the horizontal terms of PV also contribute to the change in PV and can no longer be neglected (Harvey et al., 2020; Oertel et al., 2020). In an environment with vertical wind shear, diabatic heating in convective updrafts causes horizontal dipoles of PV at mid to upper levels (Oertel et al., 2020). Therefore, the effect of convective updrafts on the distribution of PV can be seen as a tilting of the PV dipole from the vertical into the horizontal (Oertel et al., 2020). Near the convective updraft, the effect of these PV dipoles is a deceleration of the flow (Oertel et al., 2020). If the PV anomalies survive for several hours and the upper-level flow advects them downstream, they interact with and influence the large-scale circulation (Oertel et al., 2020).

During the last decades, the quality of weather and climate models increased in concert with the increase in model resolution (Düben et al., 2020). At the moment, both numerical weather prediction and climate simulation communities are making extensive efforts to refine the horizontal resolution of their models to about one kilometer to simulate convection explicitly (Schär et al., 2019). Parameterizations of sub-grid processes are a significant source of model errors, and especially convection parameterization schemes are considered a major source of uncertainties (Prein et al., 2015). Convection-permitting simulations no longer rely on parametrizing deep convection and, therefore, produce more realistic results and more reliable climate information on local to regional scales (Prein et al., 2015; Düben et al., 2020). Prein et al. (2015) also found that convection-permitting climate models represent topography and surface fields more precisely. Additionally, they state that global simulations at high resolutions are more rigorous compared to only modeling high resolution at a limited area, "as it allows for a seamless simulation of processes ranging from the scale of convective clouds to the global scale". These points are generally also applicable for numerical weather prediction. Düben et al. (2020) showed with their recent study that global convection-permitting simulations are possible today. However, they point out that, at the moment, simulations with a grid spacing of $\mathcal{O}(1\,\mathrm{km})$ still take too long, and increasing the speed by a factor of roughly 100 is needed for operational weather prediction or long-term climate simulations.

At the European Centre for Medium-Range Weather Forecasts (ECMWF), global operational medium-range weather forecasts started in 1979 with the first operational model having a resolution of about 210 km (ECMWF, 1980). In 1983, the spectral model with a grid spacing of about 1.9° was set operational (ECMWF, 1984). The ECMWF steadily reduced the grid spacing of its spectral model in the following decades, and since 2016, the high-resolution forecasts run with a grid spacing of 9 km (ECMWF, 2016). The dynamical core of the Integrated Forecasting System (IFS) at the ECMWF solves a hydrostatic set of equations. It uses spectral transform (ST) to switch between grid-point space and spectral space (ECMWF, 2020). The IFS also has a non-hydrostatic dynamical core, which is only used for research experiments (ECMWF, 2020). Despite that the current operational IFS model will remain competitive for many years, the ECMWF has developed an alternative dynamical core, the finite volume module (FVM; Kühnlein et al., 2019). The FVM shares the same set of atmospheric physics parameterizations as the ST model of the IFS. First simulations on the kilometer scale were already performed with the FVM and the ST model's non-hydrostatic option for research purposes (see, e.g., Düben et al., 2020).

The development of operational models, the subsequent increase of model resolution, and the recent progress to convection-permitting simulations also influenced the investigation of WCBs. Before WCBs were detected with the help of trajectories, Harrold (1973), Carlson (1980), and

Browning (1986) identified WCBs based on satellite images and isentropic analyses. Wernli and Davies (1997) were the first to identify WCB air-parcel in a Lagrangian analysis objectively. They and also later studies (e.g., Pomroy and Thorpe, 2000; Eckhardt et al., 2004; Grams et al., 2011; Madonna et al., 2014; Pfahl et al., 2014; Binder et al., 2016) used wind fields from reanalysis datasets or analysis data with a horizontal resolution of about 25–100 km to drive the trajectory calculations. More recent studies (e.g., Joos and Wernli, 2012; Martínez-Alvarado et al., 2014; Martínez-Alvarado and Plant, 2014) used limited-area models with higher resolutions but still parametrized convection to investigate WCBs. Most recent studies by Rasp et al. (2016), Oertel et al. (2019), and Oertel et al. (2020) used convection-permitting regional models. In these studies, they could show that potentially convective ascent in a WCB can be determined with trajectories. Oertel et al. (2019) identified in their regional convection-permitting simulation two different types of WCB trajectories: very rapidly ascending "convective" WCB trajectories and more slowly ascending "slantwise" WCB trajectories. They compared the trajectories in the convection-permitting model to WCBs in a coarser global model, which was unable to display convective ascent embedded in the WCB.

We have seen that a WCB influences the PV pattern and, consequently, dynamics of an extratropical cyclone, the precipitation pattern, and through diabatic processes also the flow evolution downstream. Convection embedded in a WCB then again alters these processes. Therefore, explicitly simulating convection and, hence, the model resolution is crucial for a WCB and its impacts. Moreover, errors in the representation of WCBs can impair the quality of the forecast downstream (Grams et al., 2011). Especially the strong diabatic processes within WCBs can lead to forecast errors (Martínez-Alvarado et al., 2016). To further investigate the dynamical effect of convection embedded in WCBs, Oertel et al. (2019) suggests a direct comparison of high-resolution convection-permitting model simulations with coarser simulations. However, no systematic analysis of the effect of model resolution on the representation of a WCB has been carried out.

2 Objectives

For the first time, this project will compare WCBs in global model simulations of different resolution in the course of a case study. We will identify and analyze the WCB based on calculated trajectories. Apart from runs with the operational IFS model at a nominal grid spacing of about 9 km, we will investigate global convection-permitting simulations with the non-hydrostatic option of the IFS ST model at a resolution of $\mathcal{O}(2\,\mathrm{km})$. This allows us to assess whether different model resolutions and explicitly representing deep convection affect the structure of the WCB and its dynamics. It is important to explore the impact of explicitly simulating deep convection on the large-scale flow evolution downstream. More precisely, this master thesis will address the following research questions:

- What is the dependency of different characteristics (such as total heating, ascent rates, outflow level) of the identified WCB on model resolution and the explicit representation of convection?
- What are the differences between the WCB-related PV anomalies at different model resolutions?
- What is the impact of high resolution on the two-day precipitation forecast associated with the WCB?
- What is the impact of high resolution on the large-scale flow evolution downstream of the WCB in the following five days?

3 Data and Methods

3.1 Data

In this master thesis, we will use forecasts from the IFS model, the numerical weather prediction model at the ECMWF. We will compare the current operational IFS model with a convection-permitting simulation of the non-hydrostatic option of the IFS. Additionally, we will use data from operational analysis as a reference state.

The operational forecast has a horizontal resolution of O1280 with 137 vertical levels. Output fields will be available every hour and are interpolated to a regular 0.1° x 0.1° grid. The model applies the operational set of physical parametrization schemes of the IFS, including deep convection.

The forecast of the global convection-permitting model simulation has a nominal horizontal resolution of about 2 km. Model output fields will be available every hour but only for a few weeks in the last decade. They will be retrieved only over a limited area of the globe (see later) and interpolated to a regular 0.02° x 0.02° grid. The retrieval and interpolation of this data will be done with the help of Nils Wedi from the ECMWF. This model version uses the ST method to solve the non-hydrostatic equations and has the parametrization for deep convection turned off (Düben et al., 2020). Otherwise, it uses the standard set of physical parameterization schemes, including shallow convection.

The IFS operational analysis has an O1280 octahedral reduced Gaussian grid with 9 km nominal horizontal grid spacing and 137 vertical levels. The fields are available every six hours and will be interpolated to a regular 0.1° x 0.1° latitude-longitude grid.

3.2 Trajectory calculation

Based on the three-dimensional wind fields of the different data sets, we will calculate trajectories with the Lagrangian analysis tool (LAGRANTO; Wernli and Davies, 1997; Sprenger and Wernli, 2015). As a first step, WCBs are identified based on trajectories in the operational analysis data. For the period where the data of the high-resolution IFS simulation is available, trajectories are started every 6 h from 0 h to 24 h and calculated 2-day forward. Trajectory starting points will be in the boundary layer (1050 hPa to 790 hPa) vertically every 20 hPa and with a horizontal grid spacing of $\delta x = 80$ km (Madonna et al., 2014). As in Madonna et al. (2014), only trajectories that ascend a pressure difference of at least 600 hPa in 48 h and can be associated with a cyclone are retained.

Based on these results, an exciting WCB and cyclone will be selected, and the area and period of the WCB case study will be defined. For further analysis, only this defined area and period will be investigated. The selected WCB should start its ascent ideally in the first hours of the two forecasts such that the forecasts at different resolutions are as identical as possible. Identical starting conditions of the WCB ascent are essential to detect just the effect of model resolution and not differing initial conditions. They also allow for exploring the downstream influence and development of the WCB.

Based on the case study definition, the data from the convection-permitting global simulation will be retrieved for the area of interest. We will further calculate trajectories in the operational forecast and then in the convection-permitting simulation. Starting points of the trajectories will be set in both forecasts in the boundary layer (1050 hPa to 790 hPa) vertically every 20 hPa with a horizontal grid spacing of $\delta x = 20$ km. We plan to start the trajectories every hour covering 6 h before to 6 h after the first and last starting time of WCB trajectories in the analysis data, respectively. The trajectories will be calculated 48 h forward. Only those trajectories that ascend

at least 600 hPa in 48 h and are associated with the chosen cyclone are retained. The selected trajectories then will be extended for three days downstream and up to the initialization time of the forecasts upstream (backward trajectory), leading to a total length of the trajectories of five to six days. Together with position (longitude, latitude) and pressure, the following variables are tracked along the trajectories: three-dimensional wind field, PV, specific humidity, and potential temperature. If available, also fields related to microphysical processes will be tracked along the trajectories.

3.3 Intercomparison

For the intercomparison of the output fields, we will coarse-grain the fields of the convection-permitting simulation to the resolution of the operational forecast. The coarse-graining is particularly crucial for fields with small features like PV. We will analyze the WCB trajectories and the related fields with horizontal cross-sections at different standard pressure levels and vertical cross-sections. For the treatment of the four questions posed in the objectives, we will apply the following methods:

The WCB intercomparison will constitute investigating location and number of trajectories as well as the evolution of the variables along the trajectories. Thereby, we will apply simple statistical measures. The hourly precipitation fields will be first compared for the entire cyclone. Additionally, we will define two-dimensional masks for every time step based on the location of the WCB trajectories. All the precipitation beneath a grid point with a trajectory will be attributed to the WCB. We will then investigate the resulting precipitation fields of the WCB with simple statistical analysis.

We will compare PV fields on low levels on different standard pressure levels and at higher elevations on isentropic surfaces. The PV fields of the convection-permitting simulation will also be investigated with the original resolution for the investigation of small-scale features like PV dipoles (cf. Oertel et al., 2020).

For the flow evolution downstream, we will compare the forecast fields with fields of the operational analysis (reference state). Besides, we will compare fields among the simulations with different resolutions. Thereby, the investigated fields are the pattern of PV on isentropic surfaces and geopotential height on 200 hPa, 300 hPa, or 200 hPa, depending on season and location of the case study. This intercomparison will be done three to six days after the main start of the WCB ascent.

4 Timeline and milestones

The master thesis will start in mid-September 2020 and be submitted at the end of March 2021. The thesis is planned in a way that each research question posed in the objectives will be investigated in roughly one month, as shown in Table 1.

Table 1: Planned timeline and milestones for the master thesis.

month	**duration**	**activity**
September	2 weeks	review literature and write introduction
October	3 weeks	define case study, calculate trajectories, get an overview of the case study, and write associated parts
Milestone I		case study defined and trajectories calculated
October & November	1 month	analyze WCB at different model resolutions and write associated parts
November & December	1 month	analyze PV anomalies related to the WCB
Milestone II		analysis of WCB and related PV anomalies completed
December & January	1 month	analyze precipitation pattern and write associated parts
January & February	1 month	analyze downstream development and write associated parts
Milestone III		analysis of precipitation pattern and downstream development completed
February & March	1 month	write the last parts of the thesis, submit the thesis for review, and revise the entire thesis
Milestone IV		master thesis submitted

5 References

Binder, H., Boettcher, M., Joos, H., and Wernli, H., 2016. The role of warm conveyor belts for the intensification of extratropical cyclones in Northern Hemisphere winter. *Journal of the Atmospheric Sciences*, 73(10), pp.3997–4020. DOI: 10.1175/JAS-D-15-0302.1.

Browning, K.A., 1971. Radar measurements of air motion near fronts. *Weather*, 26(8), pp.320–340. DOI: 10.1002/j.1477-8696.1971.tb04211.x.

Browning, K.A., 1986. Conceptual models of precipitation systems. *Weather and Forecasting*, 1(1), pp.23–41. DOI: 10.1175/1520-0434(1986)001<0023:CMOPS>2.0.CO;2.

Carlson, T.N., 1980. Airflow through midlatitude cyclones and the comma cloud pattern. *Monthly Weather Review*, 108(10), pp.1498–1509. DOI: 10.1175/1520-0493(1980)108<1498:ATMCAT>2.0.CO;2.

Carlson, T.N., 1991. *Mid-latitude weather systems*. London: HarperCollins Academic.

Crespo, J. and Posselt, D., 2016. A-Train-based case study of stratiform-convective transition within a warm conveyor belt. *Monthly Weather Review*, 144(6), pp.2069–2084. DOI: 10.1175/MWR-D-15-0435.1.

Düben, P.D., Wedi, N., Saarinen, S., and Zeman, C., 2020. Global simulations of the atmosphere at 1.45 km grid-spacing with the Integrated Forecasting System. *Journal of the Meteorological Society of Japan. Ser. II*, advpub. DOI: 10.2151/jmsj.2020-016.

Eckhardt, S., Stohl, A., Wernli, H., James, P., Forster, C., and Spichtinger, N., 2004. A 15-year climatology of warm conveyor belts. *Journal of Climate*, 17(1), pp.218–237. DOI: 10.1175/1520-0442(2004)017<0218:AYCOWC>2.0.CO;2.

ECMWF, 1980. *Annual Report 1979*. (Annual Report). Reading: ECMWF. Available from: https://www.ecmwf.int/node/16272.

ECMWF, 1984. *Annual Report 1983*. (Annual Report). Reading: ECMWF. Available from: https://www.ecmwf.int/node/16276.

ECMWF, 2016. *New forecast model cycle brings highest-ever resolution*. Available from: https://www.ecmwf.int/en/about/media-centre/news/2016/new-forecast-model-cycle-brings-highest-ever-resolution [Accessed April 22, 2020].

ECMWF, 2020. *Atmospheric dynamics*. Available from: https://www.ecmwf.int/en/research/modelling-and-prediction/atmospheric-dynamics [Accessed April 23, 2020].

Flaounas, E., Kotroni, V., Lagouvardos, K., Gray, S.L., Rysman, J.-F., and Claud, C., 2018. Heavy rainfall in Mediterranean cyclones. Part I: contribution of deep convection and warm conveyor belt. *Climate Dynamics*, 50(7), pp.2935–2949. DOI: 10.1007/s00382-017-3783-x.

Flaounas, E., Lagouvardos, K., Kotroni, V., Claud, C., Delanoë, J., Flamant, C., Madonna, E., and Wernli, H., 2016. Processes leading to heavy precipitation associated with two Mediterranean cyclones observed during the HyMeX SOP1. *Quarterly Journal of the Royal Meteorological Society*, 142(S1), pp.275–286. DOI: 10.1002/qj.2618.

Grams, C.M., Wernli, H., Böttcher, M., Čampa, J., Corsmeier, U., Jones, S.C., Keller, J.H., Lenz, C., and Wiegand, L., 2011. The key role of diabatic processes in modifying the upper-tropospheric wave guide: a North Atlantic case-study. *Quarterly Journal of the Royal Meteorological Society*, 137(661), pp.2174–2193. DOI: 10.1002/qj.891.

Harrold, T.W., 1973. Mechanisms influencing the distribution of precipitation within baroclinic disturbances. *Quarterly Journal of the Royal Meteorological Society*, 99(420), pp.232–251. DOI: 10.1002/qj.49709942003.

Harvey, B., Methven, J., Sanchez, C., and Schäfler, A., 2020. Diabatic generation of negative potential vorticity and its impact on the North Atlantic jet stream. *Quarterly Journal of the Royal Meteorological Society*, 146(728), pp.1477–1497. DOI: 10.1002/qj.3747.

Joos, H. and Forbes, R.M., 2016. Impact of different IFS microphysics on a warm conveyor belt and the downstream flow evolution. *Quarterly Journal of the Royal Meteorological Society*, 142(700), pp.2727–2739. DOI: 10.1002/qj.2863.

Joos, H. and Wernli, H., 2012. Influence of microphysical processes on the potential vorticity development in a warm conveyor belt: a case-study with the limited-area model COSMO. *Quarterly Journal of the Royal Meteorological Society*, 138(663), pp.407–418. DOI: 10.1002/qj.934.

Kühnlein, C., Deconinck, W., Klein, R., Malardel, S., Piotrowski, Z.P., Smolarkiewicz, P.K., Szmelter, J., and Wedi, N.P., 2019. FVM 1.0: a nonhydrostatic finite-volume dynamical core for the IFS. *Geoscientific Model Development*, 12(2), pp.651–676. DOI: 10.5194/gmd-12-651-2019.

Madonna, E., Wernli, H., Joos, H., and Martius, O., 2014. Warm conveyor belts in the ERA-Interim dataset (1979–2010). Part I: climatology and potential vorticity evolution. *Journal of Climate*, 27(1), pp.3–26. DOI: 10.1175/JCLI-D-12-00720.1.

Martínez-Alvarado, O., Joos, H., Chagnon, J., Boettcher, M., Gray, S.L., Plant, R.S., Methven, J., and Wernli, H., 2014. The dichotomous structure of the warm conveyor belt. *Quarterly Journal of the Royal Meteorological Society*, 140(683), pp.1809–1824. DOI: 10.1002/qj.2276.

Martínez-Alvarado, O., Madonna, E., Gray, S.L., and Joos, H., 2016. A route to systematic error in forecasts of Rossby waves. *Quarterly Journal of the Royal Meteorological Society*, 142(694), pp.196–210. DOI: 10.1002/qj.2645.

Martínez-Alvarado, O. and Plant, R.S., 2014. Parametrized diabatic processes in numerical simulations of an extratropical cyclone. *Quarterly Journal of the Royal Meteorological Society*, 140(682), pp.1742–1755. DOI: 10.1002/qj.2254.

Neiman, P., Shapiro, M., and Fedor, L., 1993. The life cycle of an extratropical marine cyclone. Part II: mesoscale structure and diagnostics. *Monthly Weather Review*, 121(8), pp.2177–2199. DOI: 10.1175/1520-0493(1993)121<2177:TLCOAE>2.0.CO;2.

Oertel, A., Boettcher, M., Joos, H., Sprenger, M., and Wernli, H., 2020. Potential vorticity structure of embedded convection in a warm conveyor belt and its relevance for large-scale dynamics. *Weather and Climate Dynamics*, 1(1), pp.127–153. DOI: 10.5194/wcd-1-127-2020.

Oertel, A., Boettcher, M., Joos, H., Sprenger, M., Konow, H., Hagen, M., and Wernli, H., 2019. Convective activity in an extratropical cyclone and its warm conveyor belt – a case-study combining observations and a convection-permitting model simulation. *Quarterly Journal of the Royal Meteorological Society*, 145(721), pp.1406–1426. DOI: 10.1002/qj.3500.

Pfahl, S., Madonna, E., Boettcher, M., Joos, H., and Wernli, H., 2014. Warm conveyor belts in the ERA-Interim dataset (1979—2010). Part II: moisture origin and relevance for precipitation. *Journal of Climate*, 27(1), pp.27–40. DOI: 10.1175/JCLI-D-13-00223.1.

Pomroy, H.R. and Thorpe, A.J., 2000. The evolution and dynamical role of reduced upper-tropospheric potential vorticity in intensive observing period one of FASTEX. *Monthly Weather Review*, 128(6), pp.1817–1834. DOI: 10.1175/1520-0493(2000)128<1817:TEADRO>2.0.CO;2.

Prein, A.F., Langhans, W., Fosser, G., Ferrone, A., Ban, N., Goergen, K., Keller, M., Tölle, M., Gutjahr, O., Feser, F., Brisson, E., Kollet, S., Schmidli, J., Lipzig, N.P.M. van, and Leung, R., 2015. A review on regional convection-permitting climate modeling: demonstrations, prospects, and challenges. *Reviews of Geophysics*, 53(2), pp.323–361. DOI: 10.1002/2014RG000475.

Rasp, S., Selz, T., and Craig, G., 2016. Convective and slantwise trajectory ascent in convection-permitting simulations of midlatitude cyclones. *Monthly Weather Review*, 144(10), pp.3961–3976. DOI: 10.1175/MWR-D-16-0112.1.

Schär, C., Fuhrer, O., Arteaga, A., Ban, N., Charpilloz, C., Di Girolamo, S., Hentgen, L., Hoefler, T., Lapillonne, X., Leutwyler, D., Osterried, K., Panosetti, D., Rüdisühli, S., Schlemmer, L., Schulthess, T., Sprenger, M., Ubbiali, S., and Wernli, H., 2019. Kilometer-scale climate models: prospects and challenges. *Bulletin of the American Meteorological Society*. DOI: 10.1175/BAMS-D-18-0167.1.

Sprenger, M. and Wernli, H., 2015. The LAGRANTO Lagrangian analysis tool - version 2.0. *Geoscientific Model Development*, 8(8), pp.2569–2586. DOI: 10.5194/gmd-8-2569-2015.

Stohl, A., 2001. A 1-year Lagrangian "climatology" of airstreams in the Northern Hemisphere troposphere and lowermost stratosphere. *Journal of Geophysical Research: Atmospheres*, 106(D7), pp.7263–7279. DOI: 10.1029/2000JD900570.

Wernli, H. and Davies, H., 1997. A Lagrangian-based analysis of extratropical cyclones. I: the method and some applications. *Quarterly Journal of the Royal Meteorological Society*, 123(538), pp.467–489. DOI: 10.1002/qj.49712353811.

Young, M.V., Monk, G.A., and Browning, K.A., 1987. Interpretation of satellite imagery of a rapidly deepening cyclone. *Quarterly Journal of the Royal Meteorological Society*, 113(478), pp.1089–1115. DOI: 10.1002/qj.49711347803.